

RSC Advances

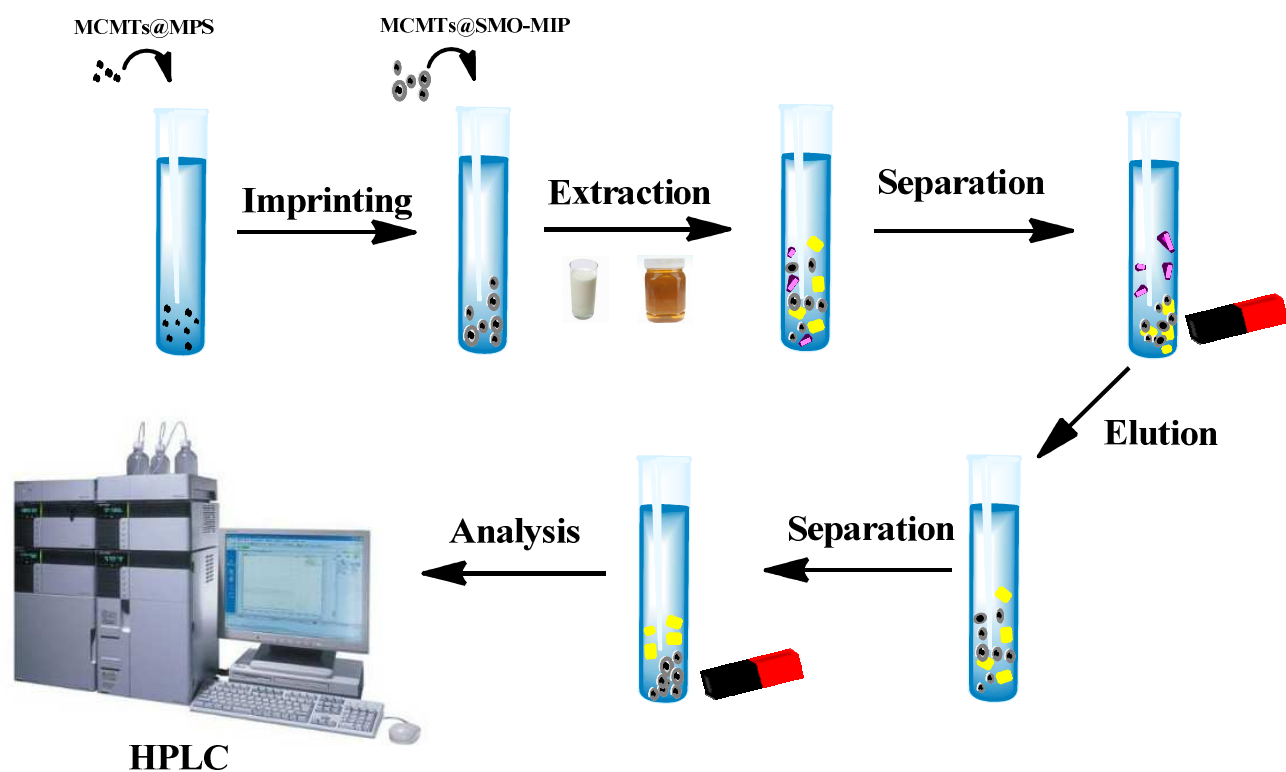


This is an *Accepted Manuscript*, which has been through the Royal Society of Chemistry peer review process and has been accepted for publication.

Accepted Manuscripts are published online shortly after acceptance, before technical editing, formatting and proof reading. Using this free service, authors can make their results available to the community, in citable form, before we publish the edited article. This *Accepted Manuscript* will be replaced by the edited, formatted and paginated article as soon as this is available.

You can find more information about *Accepted Manuscripts* in the [Information for Authors](#).

Please note that technical editing may introduce minor changes to the text and/or graphics, which may alter content. The journal's standard [Terms & Conditions](#) and the [Ethical guidelines](#) still apply. In no event shall the Royal Society of Chemistry be held responsible for any errors or omissions in this *Accepted Manuscript* or any consequences arising from the use of any information it contains.



An efficient approach was developed to synthesize the imprinted magnetic carbon nanotubes 5 nanocomposites which exhibited the considerable high binding capacity and imprinting factor. Successful application was demonstrated in the selective enrichment of SMO from milk and honey samples at low concentration levels with good recovery.



Journal Name

ARTICLE

Preparation of molecularly imprinted polymers based on magnetic carbon nanotubes for determination of sulfamethoxazole in food samples

Received 00th January 20xx,
Accepted 00th January 20xx

DOI: 10.1039/x0xx00000x

www.rsc.org/

Yingran Zhao,^{a,b} Changfen Bi,^{a,b} Xiwen He,^{a,b} Langxing Chen^{a,b,*} and Yukui Zhang^{a,b,c}

In this work, we present a general method to prepare the core-shell molecularly imprinted polymers (MIPs) on the surface of magnetic carbon nanotubes (MCNTs@MIP) for sulfamethoxazole (SMO). The resulting MCNTs@MIP possess a highly improved imprinting effect, fast adsorption kinetics and high adsorption capacity, and can be applied to fast extract sulfonamide in the milk and honey samples under an external magnetic field. The morphology, adsorption capacity and recognition properties of MCNTs@MIP composites were investigated by transmission electron microscope (TEM), fourier transform infrared (FT-IR) spectrometer, X-ray diffraction (XRD), vibrating sample magnetometer (VSM), thermogravimetric analysis (TGA), and re-binding experiments. The resulting MCNTs@MIP showed a good accessibility for the binding sites, the maximum adsorption capacity of MCNTs@MIP to SMO was 864.9 $\mu\text{g}\cdot\text{g}^{-1}$, and a high selectivity toward the template molecule (SMO) in the presence of the structural related sulfonamides (imprinting factor=10.0). A method was developed for enrichment and determination of SMO in the milk and honey samples with recoveries ranging from 68.3 to 78.2% and 73.9 to 80.1%, respectively and the relative standard deviations (RSD) (<6.8%).

1. Introduction

During recent years, antibiotics have been widely used in animal aquaculture and agricultural applications.¹ Sulfonamides (SAs), because of their physicochemical properties and broad spectrum of activity against antibacterial activity, are not only widely applied as human medicine but also used in the veterinary medicine to prevent veterinary diseases in food-producing animals.^{2,3} The residues of the drugs in foods originating from animals present a potential danger to human health (such as drug resistance, toxic effects, anaphylactic reactions, etc.).⁴ In view of these health risks, the European Commission (EC), America and other countries have adopted a maximum acceptable limit of residual sulfonamides in foods of animal origin, for example honey, milk and eggs.⁵ Therefore, it is very important to develop a versatile and sensitive analytical method for monitoring trace levels of SAs in natural product.

In the last few years, several protocols have been reported to monitor sulfonamides in food products,⁶ including high-performance liquid chromatography (HPLC), gas chromatography (GC), liquid chromatography–mass spectrometry (LC–MS), fluorometric detector

(FD) and capillary electrophoresis (CE).^{6–9} Due to the contaminants existed in food at low concentration levels, it require extensive sample preparation. As we all know, sample pretreatment is a crucial step prior to the detection of sulfonamides present in the complex matrices.¹⁰ Compared with traditional liquid–liquid extraction (LLE), solid-phase extraction (SPE) because of its advantages of rapidity, simplicity and more economical has become a routine sample preparation technique for extracting analytes. However, the LLE procedure or classical SPE have a problem that sorbents can retain other materials which can interfere with the detection of the targeted analytes.¹¹ In order to improve the selectivity, molecularly imprinted polymers (MIPs) have been used as sorbents in SPE to selectively extract analytes at low concentrations from complex matrices.^{12–17} The tailor-made recognition sites with functional and shape complementarity to the template showed the high affinity and selectivity of MIPs toward the target molecule or structural analogues.^{18,19} Molecularly imprinted solid-phase extraction (MISPE) has been widely used in environmental and complex biological samples.^{20,21} However, the MIPs synthesized by bulk polymerization exists many drawbacks, such as the heterogeneous distribution of the binding sites, slow binding kinetics, low binding capacity and selectivity, and poor site accessibility for template molecule. To solve these problems, surface imprinting on solid support^{22–25} and surface-imprinted core-shell nanoparticles^{26–31} had been developed. The introduction of the surface polymer coating on a solid support by surface imprinting technique is expected to improve the binding capacity and site accessibility of imprinted materials.

^aResearch Center for Analytical Sciences, College of Chemistry, Tianjin Key Laboratory of Biosensing and Molecular Recognition, State Key Laboratory of Medicinal Chemical Biology, Nankai University, Tianjin 300071, China

^bCollaborative Innovation Center of Chemical Science and Engineering (Tianjin), Tianjin 300071, China. Email: lxchen@nankai.edu.cn

^cDalian Institute of Chemical Physics, Chinese Academy of Sciences, Dalian 116023, P. R. China.

Nowadays, carbon nanotubes (CNTs) have been utilized for a wide variety of fields because of the observably high specific surface area, thermal, mechanical and electrical properties, such as analytical and biomedical sciences.^{32,33} To date, several MIPs for SAs such as sulfamethoxazole and sulfamethazine have been prepared as solid-phase extracting sorbents or as the stationary phase for HPLC.³⁴⁻⁴⁷ Recently, several protocols focused on analysis of sulfonamides in fish, pork, chicken and milk samples based on MIP technology have been developed. For example, Gao et al. developed the synthesis of silica-coated MIPs nanospheres for high selective extraction of sulfonamides from milk and eggs samples.³⁷ Kong et al. reported the core-shell magnetic MIPs prepared by copolymerization of vinyl grafted to the surface of Fe₃O₄ and functional monomer methacrylic acid (MAA), and applied magnetic MIPs to separate and enrich sulfamethazine from the poultry feed samples.⁴³ Dai et al. synthesized a 13 nm MIP shell through reverse atom transfer radical polymerization (RAFT), which exhibited excellent selectivity and good reuse in the analysis of sulfamethazine.⁴⁵ Mao et al. developed a surface-initiated atom transfer radical polymerization strategy for highly dense imprinting of sulfamethazine at the surface of Fe₃O₄.⁴⁷ Herein, this work represents the first attempt to prepare MIPs on the surface of magnetic carbon nanotubes (MCNTs@MIP) for highly specific enrichment and separation of sulfamethoxazole. When magnetic carbon nanotubes (MCNTs) are encapsulated into the MIP, the synthetic MCNTs@MIP can be performed easily in crude samples and separated by an external magnetic field, and several stages of sample pretreatment can be ignored including centrifugation, filtration.^{48,49} Due to the imprinted cavities, MCNTs@MIP can not only powerfully and efficiently separate procedures but also can selectively recognize the template molecules in complex matrices.⁵⁰ Therefore, the combining magnetic separation, and the more imprinted cavities within the polymer would present a powerful analytical protocol with characteristics of simplicity, selectivity and flexibility.

In this work, a core@shell nanostructured MCNTs@MIP composites for SMO was prepared by using sulfamethoxazole as a template molecule, copolymerization of vinyl end groups on the surface of MCNTs, methacrylic acid (MAA), ethylene glycol dimethacrylate (EGDMA) and azo-bis-isobutyronitrile (AIBN). The as-prepared MCNTs@MIP were characterized by Fourier transform infrared (FT-IR) spectrometer, transmission electron microscope (TEM), X-ray diffraction (XRD), vibrating sample magnetometry (VSM) and thermogravimetric analysis (TGA), respectively. The resulting imprinted materials possessed good dispersion in any solvents, favorable selectivity, high capacity and fast kinetics to uptake template molecule. A method was successfully developed for enrichment and determination of SMO in the milk and honey samples with good recoveries.

2 Experimental

2.1 Chemicals

Iron(III) chloride hexahydrate (FeCl₃·6H₂O), ethylene glycol (EG), acetic acid, disodium phosphate (Na₂HPO₄), ammonium hydroxide (NH₃·H₂O), nitric acid, ethanediamine (EDA), sodium acrylate,

methanol, anhydrous ethanol and acetonitrile were purchased from Chemicals Reagent Company (Tianjin, China). 3-Methacryloyloxypropyltrimethoxysilane (MPS), methacrylic acid (MAA), sulfamethoxazole (SMO), sulfamethazine (SMZ), sulfamerazine (SMR), sulfadimethoxine (SDM), sulfameter (SME) (Figure 1), and ethylene glycol dimethacrylate (EGDMA) were purchased from Alfa Aesar Chemical Company and azodiisobutyronitrile (AIBN) was purchased from Acros Organics (Geel, Belgium). Deionized water was prepared purchased from a Water-Pro Water System (Aquapro Corporation, AFZ-6000-U, China). Carbon nanotubes (diameters: 60–100 nm, lengths: 5–15 μm) were purchased from Shenzhen Nanotechnologies Port Co. Ltd.

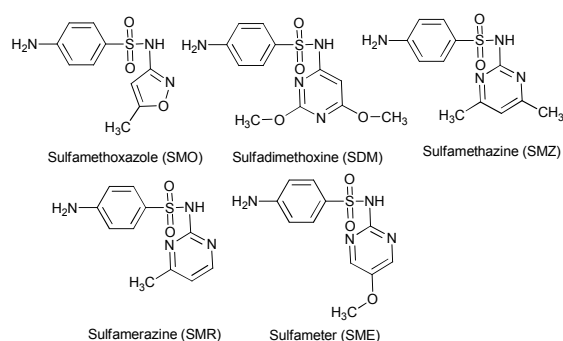


Figure 1 Molecular structure of the sulfonamides used in this work.

2.2 Synthesis of MCNTs

MCNTs were synthesized by a modified solvothermal method. Fe₃O₄ nanoparticles were generated by reduction reactions between ethylene glycol and FeCl₃ in a hydrothermal system. Typically, 40 mg of purified CNTs were dissolved in 20 mL of EG solution by sonicating for 30 min. Then 0.60 g of FeCl₃·6H₂O, 1.8 g of NaAc and 6 mL ethanediamine were dispersed in the above solution under ultrasonication. The homogenous black solution obtained was transferred to a Teflon-lined stainless-steel autoclave and maintained to heat at 200 °C for 4 h, then cooled to ambient temperature. The MCNTs composites were collected using an external magnetic field and washed several times with alcohol and highly purified water, respectively, and then dried in a vacuum at 50 °C overnight.

2.3 Synthesis of vinyl-modified MCNTs

The vinyl-modified MCNTs were synthesized according to the previous literature, using MPS by a sol-gel method without pre-coating with TEOS. MCNTs@MPS composites were synthesized generally as follows: 200 mg MCNTs was dissolved in 40 mL of ethanol in a round bottomed flask, then 10 mL of deionized water and 1.5 mL of NH₃·H₂O were added by sonicating for 30 min. Then, the mixture was stirred vigorously (600 rpm), whilst adding 300 μL of MPS drop by drop. The above mixture was reacted for 24 h at 60 °C under continuous stirring. The final products, vinyl-modified MCNTs@MPS were collected by an external magnetic field, washed

with highly purified water and methanol several times to remove the interfering substance, and dried at 50 °C in vacuum overnight.

2.4 Preparation of the core-shell MCNTs@SMO-MIP and MCNTs@NIP

The MCNTs@SMO-MIP were prepared as follows: firstly, The SMO (150 mg) as the template and MAA (225 μL) as the functional monomer were dissolved in 30 mL acetonitrile and the mixture stored in refrigerator for preparation of the preassembly solution about 12 h. Then 100 mg vinyl-modified MCNTs were dispersed into 30 mL of acetonitrile solvent, 1 mL of EGDMA and 40 mg AIBN were added into the above mixture by ultrasonic vibration for 30 min. After filled with nitrogen gas for 10 min to remove oxygen, the mixture was stirred under nitrogen following by adding the preassembly solution. The mixture was heated to reflux, with first prepolymerized at 50 °C for 6 h, then polymerized at 60 °C for 24 h, and further aged at 75 °C for 6 h. The solution was stirred at 300 rpm and purged with nitrogen gas.

After the polymerization, the MCNTs@SMO-MIP were washed with acetonitrile several times until the supernatant was clear, and the resultant products were washed with methanol-HAc (9:1, v/v) several times to remove the template molecules. Finally, the polymers were repeatedly washed with methanol, and then dried under vacuum. In parallel, non-imprinted MCNTs@NIP were prepared and processed by using a similar procedure without adding the template SMO.

2.5 Characterization

The morphology and structure of the synthesized magnetic nanocomposites were evaluated using a Tecnai G2T2 S-TWIN transmission electron microscope (TEM). Samples for TEM were prepared by placing a drop of dilute particles of solution in the ethanol solvent on a copper grid. The infrared spectra were recorded on a Nicolet AVATAR-360 Fourier transform infrared (FT-IR) spectrometer. After vacuum drying, the samples were thoroughly mixed with KBr (the weight ratio of sample/KBr was 1%) in a mortar, and then the fine powder was pressed into a pellet. The identification of the crystalline phase was performed on a Rigaku D/max/2500v/pc (Japan) X-ray diffractometer with a Cu K α source. The 2θ angles probed were from 3° to 80° at a rate of 4° min⁻¹. The magnetic properties were analyzed with a vibrating sample magnetometer (VSM) (LDJ 9600-1, USA). Thermogravimetric analysis (TGA) was performed in nitrogen atmosphere at a heating rate of 10 °C min⁻¹ from room temperature to 800 °C (NETZSCH, TG209, Germany).

2.6 HPLC analysis

HPLC analysis were performed on a Shimadzu LC-20A HPLC system including a variable wavelength UV detector (Shimadzu, Kyoto, Japan), using a Shimadzu VP-ODS C18 (5 μm particle size, 150 mm \times 4.6 mm) analytical column. The mobile phase was acetonitrile-10 mM H₃PO₄ (0-13 min (12:88, v/v), 13-30 min (12:88-30:70, v/v), 30-50 min (30:70-12:88, v/v) at a flow rate of

1.0 mL min⁻¹. The injection volume was 20 μL , and the column effluent was monitored at 270 nm.

2.7 Re-binding experiments of MCNTs@SMO-MIP and MCNTs@NIP

In adsorption kinetic experiments, 15 mg of MCNTs@SMO-MIP or MCNTs@NIP were added to 3 mL of SMO solution at a concentration of 10 $\mu\text{g}\cdot\text{mL}^{-1}$, and the specimens were incubated at a certain amount of time from 5 min to 60 min. The magnetic polymers and supernatant were separated using a permanent magnet and the concentration of the SMO in the solution was determined by HPLC analysis.

In order to investigate the adsorption equilibrium, the 15 mg of MCNTs@SMO-MIP or MCNTs@NIP were dispersed to 3 mL of acetonitrile solution of SMO with a certain concentration from 0.10 to 20 $\mu\text{g}\cdot\text{mL}^{-1}$, and the specimens were incubated for at 30 min, then the saturated magnetic polymers and supernatant were separated by an external magnet. The amount of SMO bound to the MCNTs@SMO-MIP or MCNTs@NIP in the supernatant was measured by HPLC method.

2.8 Selective enrichment and determination of SMO in the milk and honey samples

The milk and honey samples that purchased from the local retail market were selected for spiked sample analysis. 20 mL of milk sample was added into a polypropylene tube, spiked with known variable amounts of standard solution SMO and mixed with 30 mL 5% perchloric acid. The spiking concentrations for SMO were 1, 3, and 5 $\mu\text{g}\cdot\text{L}^{-1}$. The sample solution was shaken for 30 min, and then centrifugalized at 1,580 g for 10 min, the supernatant solution was filtered through a 0.22 μm filter. Removing the solvent by reduced pressure distillation, and then the residue dissolved in 20 mL acetonitrile. Next, 100 mg of MCNTs@SMO-MIP was added into the above solution, then incubated for 1 h at room temperature. After the supernatant solution were removed by a permanent magnet, 9:1 (v/v) MOH-HAc was used to wash the MCNTs@SMO-MIP composites which had absorbed the template molecule. Finally, the elution was collected, after the evaporation of the solvent by reduced pressure distillation, and the residue was concentrated with 1 mL of acetonitrile and measured by HPLC.

For honey sample analysis, firstly, 30 mL of phosphoric acid aqueous solution (pH 2.0) were added to 20 g honey sample spiked the standard SMO to give a final internal standard concentration of 1, 3 and 5 $\mu\text{g}\cdot\text{kg}^{-1}$, respectively. The SMO spiked sample solution was shaken for 30 min, and then centrifuged at 1580 g. After the supernatant solution was concentrated under reduced pressure distillation, the residue was dissolved in 20 mL acetonitrile in a polypropylene tube. An amount of 100 mg of MCNTs@SMO-MIP was put into a above polypropylene tube, then incubation for 1 h. After discarding the supernatant solution using a magnet, the MCNTs@SMO-MIP composites were washed by 9:1 (v/v) MOH-HAc to get the elution. Finally, the elute was collected and dried by rotary evaporator, and then the residue was dissolved in 1 mL acetonitrile and measured by HPLC.

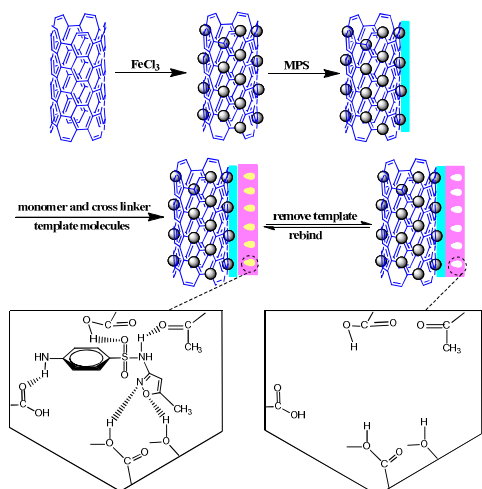


Figure 2 Scheme of synthetic route for MCNTs@SMO-MIP.

3 Results and discussion

3.1 Preparation and characterization of MCNTs@SMO-MIP nanocomposites

The synthetic strategy of MCNTs@SMO-MIP is illustrated in Figure 2. In this protocol, firstly the magnetic CNTs nanocomposite was synthesized by a modified solvothermal method.⁵¹ The surface of CNTs highly loading with Fe₃O₄ nanoparticles (NPs) was ascribed to the reductive reaction between FeCl₃ and ethylene glycol in the presence of acid-treated CNTs.⁵² Then, 3-(methacryloyloxy) propyltrimethoxysilane was directly modified to introduce active vinyl groups on the surface of MCNTs, which serve as polymerization sites in the subsequent polymerization.⁵³ Finally, MIP shell was coated onto the surface of MCNTs, after extraction of templates to generate the imprinted sites.

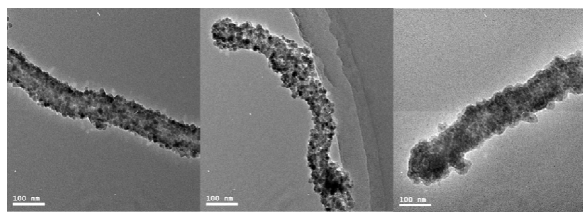


Figure 3 TEM images of MCNTs (A), MCNTs@MPS (B) and MCNTs@SMO-MIP (C).

A transmission electron microscopy (TEM) was used to check the morphological features of MCNTs, MCNTs@MPS and MCNTs@SMO-MIP. It can be seen from Figure 3, after loading with Fe₃O₄ NPs with a mean diameter of about 8 nm, the average diameter of the CNTs increased from 80 nm to approximately 96 nm, and the Fe₃O₄ NPs are well-dispersed on the surface of CNTs. When the imprinted layer had been coated on the surface of the MCNTs, the TEM image displayed that thickness of core-shell

structured MCNTs@SMO-MIP increases to approximately 110 nm (Figure 3C), corresponding to a 8-10 nm thick imprinted layer covered on MCNTs, which will be effective to the mass transport between solution and the surface of MCNTs@SMO-MIP.

The FTIR spectra of CNTs, MCNTs, MCNTs@MPS and MCNTs@SMO-MIP were displayed in Figure 4. After CNTs was purified by acid oxidation, the COO⁻ asymmetric stretching band at 1637 cm⁻¹ and O-H stretching band at 3435 cm⁻¹ obviously appeared in the spectrum of the CNTs (Figure 4A). In comparison with the infrared spectrum of the CNTs, the characteristic peak of Fe-O at 573 cm⁻¹ appears in the spectrum of the MCNTs (Figure 4B), indicating that the formation of Fe₃O₄ NPs on the surface of CNTs. The peak around 1716 cm⁻¹ in Figure 4C was assigned to the C=C stretching vibration, which indicated clearly that vinyl group was successfully modified on the surface of MCNTs. As can be seen from Figure 4D, compared with the characteristic peaks of the MCNTs@MPS, the broad absorption peak at 1253 cm⁻¹ and 1153 cm⁻¹ of MCNTs@SMO-MIP corresponded to the symmetric and asymmetric ester C-O stretching bands respectively, while the peaks of COO⁻ asymmetric stretching band at 1620 cm⁻¹ and C=O stretching band at 1731 cm⁻¹ and the C-H asymmetric stretching band at 2943 cm⁻¹, confirmed that the imprinted polymer containing methacrylic functional groups was successfully formed on the surface of MCNTs.

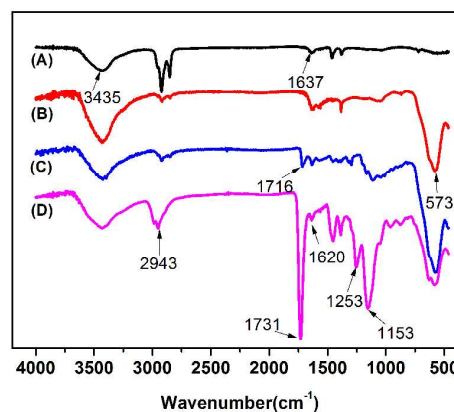


Figure 4 FT-IR spectra of CNTs (A), MCNTs (B), MCNTs@MPS (C) and MCNTs@SMO-MIP (D).

The X-ray diffraction (XRD) technique can be used to determine the crystallinity of magnetic nanocomposites. The six diffraction peaks at 30.15°, 35.54°, 43.21°, 53.41°, 57.13°, and 62.34° (Figure 5) for MCNTs, MCNTs@MPS, MCNTs@SMO-MIP are consistent with the standard XRD data of Fe₃O₄ NPs (JCPDS card no. 19-629), which were indexed as (220), (311), (400), (422), (511) and (440), respectively. The crystallinity structure did not change during the whole chemical modification reaction. And the diffraction peak at 2θ=25.16° can be indexed to the (002) observed for the CNTs.⁵⁴ As shown in the Figure 5D, the intensities of the characteristic peaks are decreased due to the imprinted polymer layer. The results showed that the crystal structure of the magnetic component was unchangeable during the whole modification process.

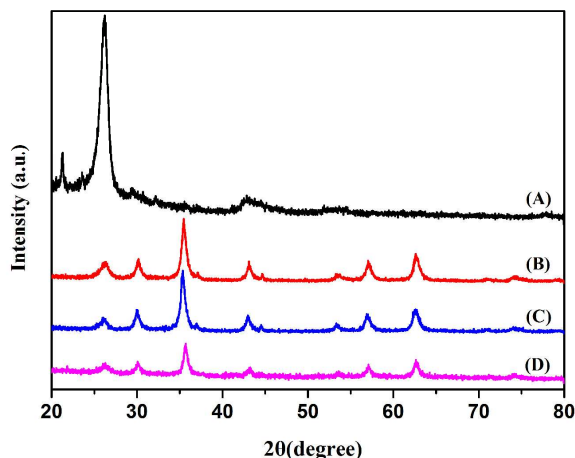


Figure 5 XRD patterns of CNTs (A), MCNTs (B), MCNTs@MPS (C) and MCNTs@SMO-MIP (D).

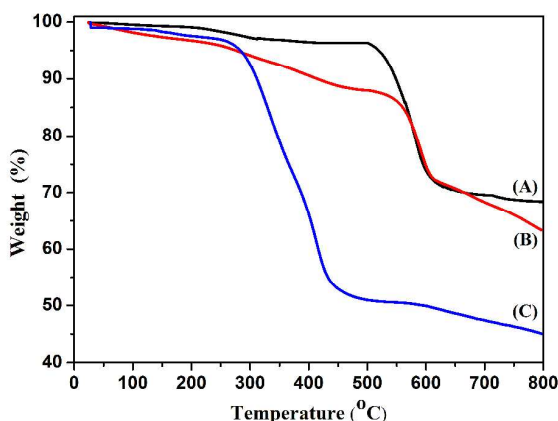


Figure 6 TGA weight loss curves of MCNTs (A), MCNTs@MPS (B) and MCNTs@SMO-MIP (C).

Thermogravimetric analysis (TGA) was performed to investigate the composition of MCNTs@SMO-MIP. As shown in Figure 6, there were two weight loss stages when the samples were heated from room temperature to 800 °C. The small weight loss of less than 5% at a temperature less than 200°C was assigned to the elimination of water or solvent. Besides, the weight of MCNTs (curve A) declined sharply between 500°C and 650°C corresponding to the decomposition of CNTs, and the remaining magnetite weight is around 70 wt% and stay constant at the temperature more than 700°C. There is about 5 wt % weight loss was observed for MCNTs@MPS due to the decomposition of grafted MPS (curve B). It can be seen that there is a very sharp weight loss (40 wt %) between 300°C and 450°C for MCNTs@SMO-MIP (curve C), which imply that the imprinted layer was approximately 21 wt % and the remaining magnetic content is around 45 wt% in MCNTs@SMO-MIP.

The magnetic properties of MCNTs, MCNTs@MPS and MCNTs@SMO-MIP were measured using a vibrating sample

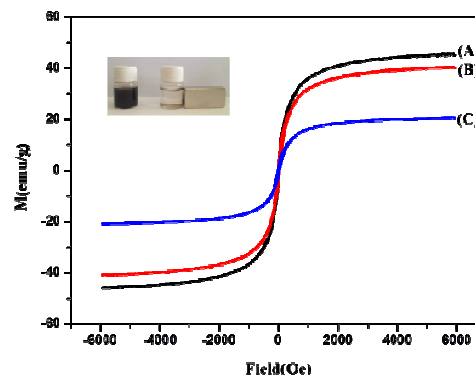


Figure 7 Magnetization curves of MCNTs (A), MCNTs@MPS (B) and MCNTs@SMO-MIP (C). Inset: the magnetic Separation of MCNTs@SMO-MIP within 60 seconds using an external magnet.

magnetometer (VSM). Typical hysteresis loops of the as-prepared nanocomposites are shown in Figure 7. Notably, there is no hysteresis for three magnetic curve suggesting that they are superparamagnetism at room temperature. The saturation magnetization (M_s) values are about 45.5, 40.5 and 20.7 $\text{emu}\cdot\text{g}^{-1}$ for MCNTs, MCNTs@MPS and MCNTs@SMO-MIP, respectively. There is no obvious decrease in the saturation magnetization (M_s) of MCNTs@MPS after modifying MPS on the surface of the MCNTs, while a great decrease after coating of the imprinted layer. The saturation magnetization of MCNTs@SMO-MIP were reduced by 24.8 $\text{emu}\cdot\text{g}^{-1}$ compared with the MCNTs, but the composites still performed strongly magnetic strength at room temperature and allowed for effective magnetic separation by the external magnetic field and can be used as a magnetic carriers. As shown in inset of Figure 7, a dark homogeneous solution existed after dispersing the composites by slight shaking in water, and they could become clear and transparent by an external magnet within several seconds, which indicates that the magnetic MCNTs@SMO-MIP can be performance for effective separation of the target molecules.

3.2 Binding characteristics of the imprinted magnetic nanocomposites

3.2.1 Adsorption of MCNTs@SMO-MIP and MCNTs @NIP

The Figure 8 presents the adsorption kinetics behavior of a 10 $\mu\text{g}\cdot\text{mL}^{-1}$ SMO solution onto the MCNTs@SMO-MIP and MCNTs@NIP. It can be seen that the adsorption capacity increased rapidly in the first 10 min and approximately reached adsorption equilibrium at 20 min for templates. Such an equilibrium time indicates that the extraction is a fast process, and 30 min was chosen as optimal adsorption time in the later work. Usually, it would take 12-24 h for traditionally imprinted materials to reach adsorption equilibrium.²⁵ However, the surface imprinting technique improves the binding kinetics and takes generally 15-200 min to reach adsorption equilibrium. Herein, the equilibrium time of MCNTs@SMO-MIP is required only about 20 min to reach equilibrium for SMO, which is superior to other surface imprinted polymers for SAs. This makes it be a time-saving method to apply for the practical analysis. The result justly demonstrated that the uniform thin imprinted layer on the surface of MCNTs shows the

advantage of faster mass transfer and binding kinetics and overcome some disadvantage of the traditionally imprinted process.

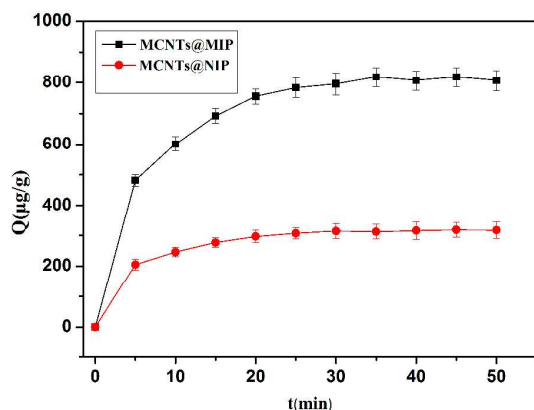


Figure 8 Adsorption kinetics curve of MCNTs@SMO-MIP and MCNTs@NIP.

The static binding tests for SMO onto MCNTs@SMO-MIP and MCNTs@NIP were investigated in the concentration range of 0.10–20 $\mu\text{g}\cdot\text{mL}^{-1}$ (initial concentration) (Figure 9A). It can be seen that the amounts of template SMO bound to the MIPs increased with increasing initial concentration and reach saturation when the initial concentration was above 10 $\mu\text{g}\cdot\text{mL}^{-1}$. In contrast, the amount of SMO bound to NIP was the lower than that of MIPs which implies that the MIPs have high specific sites for the template molecule. Furthermore, we also synthesized the imprinted and non-imprinted polymers-coated on the magnetic Fe_3O_4 NPs using the same polymerization for comparison. The adsorption of Fe_3O_4 @MIP, and Fe_3O_4 @NIPs towards SMO was shown in Figure 9B. It was found that the amount of SMO bound to Fe_3O_4 @MIPs was dramatically higher than for Fe_3O_4 @NIPs. The two non-imprinted polymers Fe_3O_4 @NIPs and MCNTs@NIP showed nearly the same binding capacity, but MCNTs@SMO-MIP has binding capacity has been increased to 1.6 times as compared with Fe_3O_4 @MIP. This demonstrated that the MCNTs is more suitable support for surface imprinting to avoid the aggregation of Fe_3O_4 @MIP.

In order to further estimate the binding properties of MCNTs@SMO-MIP, the saturation binding data were analyzed using the Langmuir isotherm model based on the following equation:

$$[\text{SMO}]/Q = 1/(Q_{\text{max}} K_{\text{D}}) + [\text{SMO}]/Q_{\text{max}} \quad (1)$$

where Q was the amount of SMO bound to the imprinted polymers at equilibrium, Q_{max} is the apparent maximum adsorption capacity, $[\text{SMO}]$ is the free concentration of SMO at equilibrium in the solution and K_{D} is the dissociation constant. The Q_{max} and K_{D} can be calculated from the intercept and slope of the linear plotted in $[\text{SMO}]/Q$ versus $[\text{SMO}]$.

The Langmuir analysis curve of MCNTs@SMO-MIP was plotted in Figure 9C. According to Langmuir model, the adsorption performs uniformly on the active sites of the adsorbent. Once the template molecules occupy the binding sites, the sites will not adsorb template molecules further. The linear regression equation for the linear region is $[\text{SMO}]/Q = 0.00551 + 0.00116[\text{SMO}]$ ($r = 0.9965$). According to the slope and the intercept obtained, the values K_{D} and

Q_{max} of MCNTs@SMO-MIP were calculated to be 0.21 $\text{mL}\cdot\mu\text{g}^{-1}$ and 864.9 $\mu\text{g}\cdot\text{g}^{-1}$ respectively. The resulting binding capacity is not expected high like carbon nanotube-based materials which usually have high specific surface area and adsorption ability, but the amount of SAs bound to MCNTs@SMO-MIP was higher than that of core-shell MIPs-coated Fe_3O_4 magnetic NPs for sulfamethazine^{43,44} and sulfamethoxazole.⁴⁷ The reason is that 10 nm imprinted layer on the surface of MCNTs sacrifices the adsorption capacity and greatly improves the selectivity of target molecules.

3.2.2 Adsorption selectivity of MCNTs@SMO-MIP towards SAs

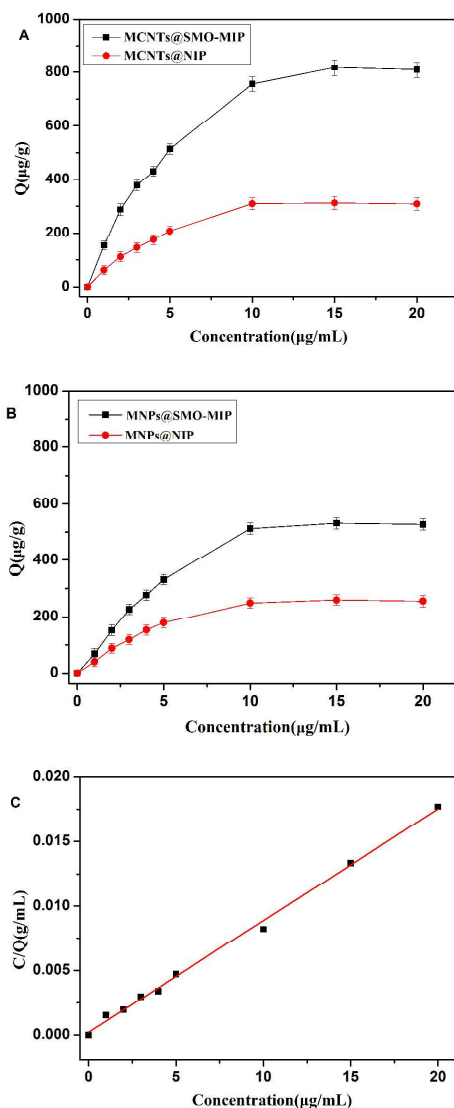


Figure 9 Adsorption isotherm of MCNTs@SMO-MIP and MCNTs@NIP (A); Fe_3O_4 @MIP and Fe_3O_4 @NIP (B). Langmuir plot to estimate the binding mechanism of MCNTs@SMO-MIP towards SMO.

In order to verify that synthesized MCNTs@SMO-MIP is selective for extraction of SMO, four other sulfonamides (SMZ, SMR, SDM and SME) were then selected to test the adsorption properties as structure analogues (Figure 1). The adsorption amounts of the

MCNTs@SMO-MIP and MCNTs@NIP towards five sulfonamides are obtained at the concentration of $10 \mu\text{g}\cdot\text{mL}^{-1}$ respective in 5 mL of acetonitrile (Figure 10). It can be seen that the amount of SMO bound to MIP was the biggest among the five SAs and was decreased to $408.5 \mu\text{g g}^{-1}$ in comparison with only SMO of $756.4 \mu\text{g g}^{-1}$ in solution. The results are ascribed to SMZ, SDZ, SMR and SME possess the closer structure, which competitively occupied the imprinted sites.

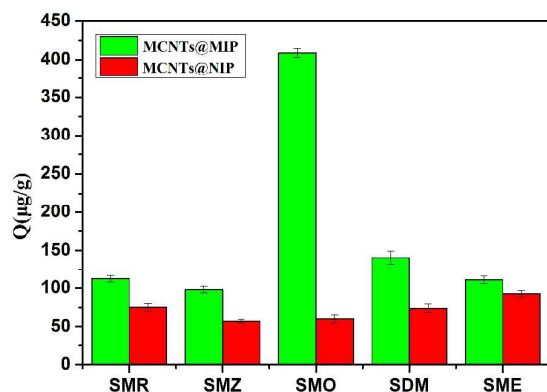


Figure 10 Adsorption capacity of imprinted and non-imprinted polymers towards SMR, SMZ, SMO, SDM and SME at a concentration of $10 \mu\text{g}\cdot\text{mL}^{-1}$ for each compound in the solution.

Table 1 The partition coefficients, binding capacity, imprinting factors and selectivity coefficients of SMO and its analogues for the imprinted and control NPs.^[a]

Analyte	$Q_{\text{MIP}}^{[b]} (\mu\text{g g}^{-1})$	$Q_{\text{NIP}}^{[b]} (\mu\text{g g}^{-1})$	$K_{\text{MIP}} (\text{mL g}^{-1})$	$K_{\text{NIP}} (\text{mL g}^{-1})$	IF	α
SMO	408.5	41.3	10.30	1.03	10.0	--
SMR	112.1	49.1	2.83	1.23	2.3	4.3
SMZ	98.1	57.2	2.48	1.42	1.7	5.9
SDM	140.7	73.8	3.54	1.84	1.9	5.3
SME	110.8	72.9	2.77	1.82	1.5	6.7

[a] In this experiment, 15 mg of the imprinted and control nanocomposites were incubated in the mixing solution of SMO, SMZ, SME, SDM and SMR at a concentrations of $10 \mu\text{g mL}^{-1}$ for 30 min at 25°C ($n=3$).

[b] Corner marks MIP and NIP represent the imprinted and control NPs respectively.

In this work, the partition coefficient, imprinting factor (IF) and selectivity coefficient (α) were used to evaluate the imprinting effect and selectivity properties of MIP and NIP toward template and other SAs with the similar structure. The partition coefficient K is calculated according to the following formula, which is defined as the adsorbed to unadsorbed concentration ratio:

$$K = C_p / C_s \quad (2)$$

Where C_p is the adsorbed concentration of test analytes, while C_s is the concentration of test analytes remaining in solution.

Additionally, the imprinting factor (IF) and the selectivity factor (α) were calculated according to the following formulas:

$$\text{Imprinting factor (IF)} = K_i / K_c \quad (3)$$

$$\text{Selectivity factor } (\alpha) = \text{IF}_{\text{SMO}} / \text{IF}_i \quad (4)$$

Where K_i and K_c represent the partition coefficients of the MCNTs@SMO-MIP toward the analytes and structural analogues. IF_{SMO} and IF_i are the imprinting factor of SMO and its similarly structured compounds, respectively.

The obtained partition coefficients, binding capacity, imprinting factors and selectivity coefficients of SMO and its analogues for the imprinted and control NPs are listed in Table 1. It can be seen from Figure 10 and Table 1, the binding amount of SMO for MCNTs@SMO-MIP is much higher than those of four other sulfonamides, meaning that imprinted polymer has a relatively higher affinity to the template molecule than its analogues. Moreover, the IF of SMO is also much higher than those of other sulfonamides. This is due to the cavities and specific binding sites existed in the MCNTs@SMO-MIP are complementary in structure, distinct size and spatial distribution with template molecule. As can be seen from Figure 1, the five sulfonamides are similarly structured compounds, which has the same sulfa group ($\text{NH}_2\text{C}_6\text{H}_4\text{NH}$). However, the difference is that SDM, SMZ, SMR, SME all have two N atoms in the pyrimidine ring while SMO has one N atom and one O atom in the oxazole ring. We can find that

the IF of SMO in the structural analogues mixed solution is obviously higher than that in only SMO solution. The results are probably attributed to the competition effects among five sulfonamides in both imprinted and non-imprinted polymers, which led to the decrease of adsorption of five sulfonamides. In addition, the template molecule has high adsorbed amount, because the interaction between polymer matrix and target was not only based on hydrogen bonding but also complementary to target in size and shape about the SMO template. The adsorption of the five compounds on MCNTs@NIP is nonspecific because of lacking the imprinting process.

Table 2 Recoveries of SMO in the spiked milk and honey samples (n=5).

samples	1.0 $\mu\text{g}\cdot\text{L}^{-1}$		3.0 $\mu\text{g}\cdot\text{L}^{-1}$		5.0 $\mu\text{g}\cdot\text{L}^{-1}$	
	Recovery (%)	RSD (%)	Recovery (%)	RSD (%)	Recovery (%)	RSD (%)
milk	68.3	6.8	74.6	4.7	78.2	4.1
honey	73.9	6.5	77.2	4.8	80.1	3.2

The IF for binding SMO was 10.0, and is also greatly higher than that of the surface imprinting technology for sulfonamides MIPs on the silica.^{37,41,42,44} It is a little higher than the MIPs-coated Fe_3O_4 NPs using the similar method as this work,⁴³ but value of IF is lower than the strategy for preparing MIP using atom transfer radical polymerization (ATRP) on the surface of Fe_3O_4 NPs.⁴⁷ The binding capacity is $408.5 \mu\text{g g}^{-1}$, which is the biggest among the MIPs for sulfonamides in the surface imprinting. These results further verified the satisfactory imprinting efficiency of the present method for preparation of MIP-coated MCNTs.

3.2.3 Reusability of SMO imprinted nanocomposites

To examine the reusability of MCNTs@SMO-MIP, the adsorption/desorption cycles were repeated for 5 times. For each adsorption/desorption cycle, the solution of milk or honey samples was extracted by MCNTs@SMO-MIP, and the MCNTs@SMO-MIP adsorbed SMO was eluted with $\text{CH}_3\text{OH-HAc}$ (v/v, 9:1). The elute was collected, evaporation and fixed constant volume for HPLC analysis. The magnetic composites could be used for five cycles with a loss of less than 7.1% on average. The result suggested that the adsorbents show good resistance for real samples analysis.

3.3 Selective enrichment and determination of SMO in milk and honey samples

The as-prepared MCNTs@SMO-MIP was applied for determination of SMO in milk and honey samples purchased from the local market. After the acetonitrile solution of milk or honey samples was extracted by MCNTs@SMO-MIP and MCNTs@NIP, the adsorbed MCNTs@SMO-MIP and MCNTs@NIP to SMO template washed with 9:1 (v/v) methanol-HAc and elutes were analyzed by HPLC. The chromatograms of spiked milk and honey samples before and after treated by MCNTs@SMO-MIP and MCNTs@NIP are displayed in Figure 11. The peaks of SMO could not be observed in the milk and honey samples spiked with SMO at a concentration of $1 \mu\text{g}\cdot\text{L}^{-1}$. After the enrichment of spiked milk and honey samples with MCNTs@SMO-MIP, the peaks of SMO appeared obviously at 10.6 min and the majority of interfering compounds in the samples were nearly eliminated. The results demonstrated that SMO spiked milk or honey could be selectively enriched by the MCNTs@SMO-MIP composites and could be recovered by the washing. It was observed that an efficient enrichment of SMO by MCNTs@SMO-MIP in comparison with MCNTs@NIP as adsorbent. The results confirmed that the prepared MCNTs@SMO-MIP could be applied to the enrichment of target analyte in the complex samples.

The analytical merit for quantitative determination of SMO via off-line MISPE-HPLC was performed by constructing the calibration curve by injecting of $20 \mu\text{L}$ standard solutions of the analyte. The calibration curve was calculated at a range of $0.050\text{--}20 \mu\text{g}\cdot\text{mL}^{-1}$, and the regression coefficient (r^2) was 0.9997. The limit of detection (LOD), calculated as the concentration corresponding to a signal-to-noise ratio (S/N) of 3, was $6.04 \mu\text{g L}^{-1}$ for SMO.

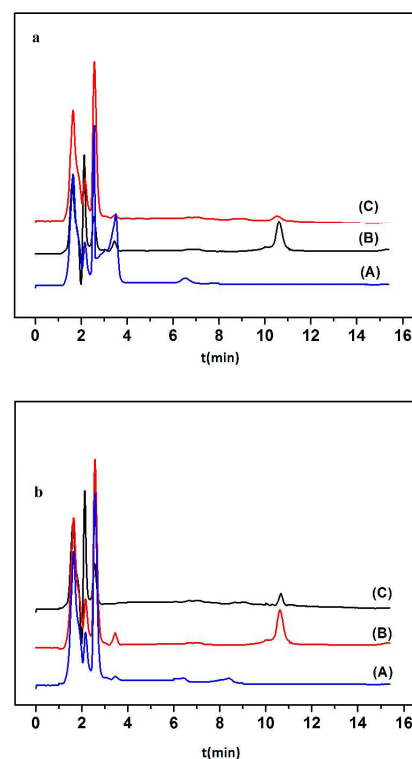


Figure 11 HPLC chromatograms of spiked milk (a) and honey (b) samples before (A) and after treated by MCNTs@SMO-MIP (B) and MCNTs@NIP (C). Samples spiked with SMO at a concentration of $1.0 \mu\text{g L}^{-1}$, elution of the MCNTs@SMO-MIP with 9:1 (v/v) $\text{CH}_3\text{OH-HAc}$.

In order to evaluate the performance of the developed method, the recoveries of SMO in the spiked milk and honey samples with three levels of SMO (1.0 , 3.0 and $5.0 \mu\text{g L}^{-1}$) were analyzed. At each concentration, five measurements were performed (Table 2). The reproducibility of the method was determined. For each concentration level, the recoveries of milk and honey samples ranged from 68.3% to 78.1% and from 73.9% to 80.1% for SMO extraction,

respectively. The relative standard deviations (RSD, $n=5$) were less than 6.8%.

4 Conclusions

In this work, we developed an efficient strategy to prepare the SMO-imprinted magnetic carbon nanotubes. The resulting MCNTs@SMO-MIP showed the improved binding capacity ($Q_{\max} = 864.9 \mu\text{g g}^{-1}$), a considerable high imprinting factor ($IF=10.0$), a fast kinetics with only 30 min to reach adsorption equilibrium and can be easily isolated from the real samples under an external magnet. Using the MCNTs@SMO-MIP nanocomposite as an absorbent, an off-line MISPE-HPLC method was presented. Successful application in the selective separation and enrichment of SMO from milk and honey samples at low concentration levels ($1.0 \mu\text{g L}^{-1}$) and good recovery were achieved after a reasonably mild elution. It was expected that the designed MIPs-coated magnetic carbon nanotubes could be an alternative solution for selective enrichment of antibiotic residuals in a complex matrix like environmental, food, feed and biological samples.

Acknowledgements

The authors are grateful to the National Basic Research Program of China (No. 2012CB910601), the National Natural Science Foundation of China (No. 21275080, 21475067), Research Fund for the Doctoral Program of Higher Education of China (No. 20120031110007) and the National Natural Science Foundation of Tianjin (No. 15JCYBJC20600).

Notes and references

- C. W. Knapp, W. Zhang, B. S. Sturm and D. W. Graham, *Environ. Pollut.*, 2010, **158**, 1506.
- C. Cháfer-Pericás, Á. Maquieira and R. Puchades, *TrAC Trends Anal. Chem.*, 2010, **29**, 1038.
- M. R. Payan, M. A. B. Lopez, R. Fernandez-Torres, M. V. Navarro and M. C. Mochon, *J. Chromatogr. B*, 2011, **879**, 197.
- A. M. Bueno, A. M. Contento and A. Rios, *J. Sep. Sci.*, 2014, **37**, 382.
- N. Furusawa, *Anal. Chimica Acta*, 2003, **481**, 255.
- S. G. Dmitrienko, E. V. Kochuk, V. V. Apyari, V. V. Tolmacheva and Y. A. Zolotov, *Anal. Chimica Acta*, 2014, **850**, 6.
- A. Fernández-González, L. Guardia, R. Badia-Lainó, M. E. Díaz-García, *TrAC Trends Anal. Chem.*, 2006, **25**, 949.
- A. Preechaworapun, S. Chuanuwatanakul, Y. Einaga, K. Grudpan, S. Motomizu and O. Chailapakul, *Talanta*, 2006, **68**, 1726.
- S. Borrás, R. Companyo, J. Guiteras, J. Bosch, M. Medina and S. Termes, *Anal. Bioanal. Chem.*, 2013, **405**, 8475.
- L. Chen, D. Song, Y. Tian, L. Ding, A. Yu and H. Zhang, *TrAC Trends Anal. Chem.*, 2008, **27**, 151.
- R. Mohamed, J. Richoz-Payot, E. Gremaud, P. Mottier, E. Yilmaz, J.-C. Tabet and P. A. Guy, *Anal. Chem.*, 2007, **79**, 9557.
- L. Chen, B. Li, *Anal. Methods*, 2012, **4**, 2613.
- Z. Xu, G. Fang and S. Wang, *Food Chem.*, 2010, **119**, 845.
- C. Baggiani, L. Anfossi, C. Giovannoli, *Anal. Chim. Acta*, 2007, **591**, 29.
- X. Hu, J. Pan, Y. Hu and G. Li, *J. Chromatogr. A*, 2009, **1216**, 190.
- X. L. Sun, X.W. He, Y. K. Zhang, L. X. Chen, *Talanta*, 2009, **79**, 926.
- F. Wei, Y. Q. Feng, *Anal. Methods*, 2011, **3**, 1246.
- M. Yan, O. Ramström, *Molecularly Imprinted Materials: Science and Technology*, Marcel Dekker, New York, 2005.
- L. X. Chen, S. F. Xu, J. H. Li, *Chem. Soc. Rev.*, 2011, **40**, 2922.
- J. Yin, Z. Meng, M. Du, C. Liu, M. Song and H. Wang, *J. Chromatogr. A*, 2010, **1217**, 5420.
- X. T. Shen, L. H. Zhu, N. Wang, L. Ye, H. Q. Tang, *Chem. Commun.*, 2012, **48**, 788.
- E. Yilmaz, K. Haupt, K. Mosbach, *Angew. Chem. Int. Ed.*, 2000, **39**, 2115.
- A. Bossi, S. A. Piletsky, E.V. Piletska, P. G. Righetti, A. P. F. Turner, *Anal. Chem.*, 2001, **73**, 5281.
- Y. Li, H. H. Yang, Q. H. You, Z. X. Zhuang, X. R. Wang, *Anal. Chem.*, 2006, **78**, 317.
- L. Li, X. W. He, L. X. Chen, Y. K. Zhang, *Chem. Asian. J.*, 2009, **4**, 286.
- S. R. Carter, S. Rimmer, *Adv. Funct. Mater.*, 2004, **14**, 553.
- C.H. Lu, W. H. Zhou, B. Han, H. H. Yang, X. Chen, X.R. Wang, *Anal. Chem.*, 2007, **79**, 5457.
- D. M. Gao, Z. P. Zhang, M. H. Wu, C. G. Xie, G. J. Guan, D. P. Wang, *J. Am. Chem. Soc.*, 2007, **129**, 7859.
- X. Wang, L.Y. Wang, X. W. He, Y. K. Zhang, L. X. Chen, *Talanta*, 2009, **78**, 327.
- R. X. Gao, X. Kong, X. Wang, X. W. He, L. X. Chen, Y. K. Zhang, *J. Mater. Chem.*, 2011, **21**, 17863.
- M. Zhang, X. H. Zhang, X. W. He, L. X. Chen, Y. K. Zhang, *Nanoscale*, 2012, **4**, 3141.
- A. Bianco, K. Kostarelos, C. D. Partidos and M. Prato, *Chem. Commun.*, 2005, 571.
- C. Staii and A. T. Johnson, *Nano Lett.* 2005, **5**, 1774.
- N. Zheng, Y. Z. Li, M. J. Wen, *J. Chromatogr. A*, 2004, **1033**, 179.
- X. J. Liu, C. B. Ouyang, R. Zhao, D. H. Shangguan, Y. Chen, G. Q. Liu, *Anal. Chim. Acta*, 2006, **571**, 235.
- M. Valtchev, B. S. Palm, M. Schiller, U. Steinfeld, *J. Hazard. Mater.*, 2009, **170**, 722.
- R. X. Gao, J. J. Zhang, X. W. He, L. X. Chen, Y. K. Zhang, *Anal. Bioanal. Chem.*, 2010, **398**, 451.
- L. G. Chen, X. P. Zhang, L. Sun, Y. Xu, Q. L. Zeng, H. Wang, H. Y. Xu, A. Yu, H. Q. Zhang, L. Ding, *J. Agric. Food Chem.*, 2009, **57**, 10073.
- M. P. Davies, V. D. Biasi, D. Perrett, *Anal. Chim. Acta*, 2004, **504**, 7.
- A. Guzmán-Vázquez de Prada, P. Martínez-Ruiz, A.J. Reviejo, J.M. Pingarrón, *Anal. Chim. Acta*, 2005, **539**, 125.
- J. X. He, S. Wang, G. Z. Fang, H. P. Zhu, Y. Zhang, *J. Agric. Food Chem.*, 2008, **56**, 2919.
- S. F. Su, M. Zhang, B. L. Li, H. Y. Zhang, X. C. Dong, *Talanta*, 2008, **76**, 1141.
- X. Kong, R.X. Gao, X.W. He, L.X. Chen, Y.K. Zhang, *J. Chromatogr. A*, 2012, **1245**, 8-16.
- S. L. Qin, S. Deng, L. Q. Su, P. Wang, *Anal. Methods*, 2012, **4**, 4278-4283.
- M. Díaz-Álvarez, F. Barahona, E. Turiel, A. Martín-Esteban, *J. Chromatogr. A*, 2014, **1357**, 158-164.
- J. D. Dai, Z.P. Zhou, Y.L. Zou, *J. Appl. Polym. Sci.*, 2014, **131**, 40854.
- X. D. Mao, H. Y. Sun, X. W. He, L. X. Chen, Y. K. Zhang, *Anal. Methods*, 2015, **7**, 4707-4716.
- L. Chen, T. Wang, J. Tong, *TrAC Trends Anal. Chem.* 2011, **30**, 1095.
- K. Aguilar-Arteaga, J. A. Rodriguez, E. Barrado, *Anal. Chim. Acta*, 2010, **674**, 157.
- J. M. Pan, H. Yao, L. C. Xu, H. X. Ou, P.W. Huo, X. X. Li, Y. S. Yan, *J. Phys. Chem. C*, 2011, **115**, 5440.
- Y. Zhang, Z. Y. Hu, H. Q. Qin, X. L. Wei, K. Cheng, F. J. Liu, R. A. Wu and H. F. Zou, *Anal. Chem.*, 2012, **84**, 10454.
- R. X. Gao, X. Q. Su, X. W. He, L. X. Chen, Y. K. Zhang, *Talanta*, 2011, **83**, 757.
- X. H. Zhang, X. W. He, L. X. Chen and Y. K. Zhang, *J. Mater. Chem.*, 2012, **22**, 16520.
- B. P. Jia, L. Gao, J. Sun, *Carbon*, 2007, **45**, 1476.